ELSEVIER

Biophysical Chemistry 63 (1997) 133–146

Biophysical Chemistry

Electron transfer between myoglobin and electrodes in thin films of phosphatidylcholines and dihexadecylphosphate

Zhe Zhang, James F. Rusling *

Department of Chemistry, Box U-60, University of Connecticut, Storrs, CT 06268-4060, USA

Received 3 June 1996; revised 26 August 1996; accepted 26 August 1996

Abstract

Myoglobin (Mb) in thin films of phosphatidyl cholines (PC) or dihexadecyl phosphate (DHP) gave direct, reversible electron transfer between pyrolytic graphite electrodes and the heme Fe(III)/Fe(II) redox couple of the protein. PC films incorporated much more Mb than DHP films. A model assuming several classes of electroactive sites in the films on the electrode with a dispersion of standard potentials successfully fit square-wave voltammetric data at pulse heights > 50 mV. Electron transfer rate constants in PC and DHP films were significantly larger than for Mb in thin films of an insoluble cationic surfactant. The pH dependence of the formal potential of Mb in the PC films suggested that protonation, possibly inducing conformational change, accompanies electron transfer to MbFe(III) between pH 5 and 11. Mb in PC films was used for catalysis of the reduction of trichloroacetic acid.

Keywords: Myoglobin; Phosphatidylcholine; Electron transfer; Thin protein films; Models for square wave voltammetry; Catalysis

1. Introduction

While primarily an oxygen transport protein in mammalian muscle, the heme protein myoglobin (Mb) can also act as an oxidation [1,2] or a reduction [3–5] catalyst. In this respect, it has similar properties to cytochrome P450, which catalyzes organic oxidations and reductions, and is implicated in carcinogenic activation of pollutants in living systems [6–8]. While myoglobin is less stereo- and regioselective in most of its catalytic reactions, it provides a readily available model for investigation of possible chemical pathways of pollutant activation. Furthermore, lipid peroxidation catalyzed by myoglobin may be important in myocardial reperfusion damage [9–12].

As with the cytochromes P450 [13–15], electron transfer to the Fe(III) form of myoglobin is the initial step in its catalytic cycles [1–5]. For catalytic reductions, this first electron transfer occurs under anaerobic conditions. Catalytic oxidations require oxygen and additional electron transfer steps.

We recently reported direct electron transfer between electrodes and aquo-metmyoglobin, i.e., the Fe(III) form of Mb with water as an axial ligand, in films of insoluble surfactants [5]. In contrast, this electrochemical reduction has been obtained in solution only with highly purified Mb on specially cleaned "hydrophilic" tin-doped indium oxide electrodes [16–18]. Electron transfer rates in liquid crys-

* Corresponding author.

PII S0301-4622(96)02216-8

tal films of lipid-like surfactants [5,18–20] were 10-fold larger than for ultrapure Mb in water on the "hydrophilic" indium oxide electrodes, and over 1000-fold larger than on Au, Pt, and carbon electrodes.

Cationic and nonionic surfactants and cationic surfactants with polymeric anions have been used to make stable films with Mb [5,18–20]. All the surfactants have two or three long hydrocarbon tails. They self-assemble into multiple bilayer structures similar to lipid bilayers and exhibit characteristic gel-to-liquid crystal phase transitions. ESR anisotropy and linear dichroism showed that Mb is specifically oriented in these films [5,20,21]. Comparable electron transfer rates were found for all of these films in their liquid crystal states. Mb–surfactant films on electrodes were recently used to catalyze reduction of organohalide pollutants [22] mimicking cytochrome P450 in an anaerobic environment.

In this paper, we describe the electrochemical properties of Mb in films of phosphatidyl cholines (PC), of particular interest as components of biological membranes [23,24]. We also report studies of Mb in films of dihexadecyl phosphate (DHP) as an example of an anionic surfactant, which has not been employed previously. Square wave voltammograms of these films were successfully modeled by assuming a dispersion of standard potentials for Mb in the films.

2. Experimental section

2.1. Materials and apparatus

Myoglobin from horse skeletal muscle (Sigma) was dissolved in water or buffer and passed through Amicon YM30 filters (30,000 MW cutoff) [11]. Concentrations after ultrafiltration were estimated by spectroscopy [5]. Buffers were 0.01 M tris(hydroxymethyl)aminomethane · HCl (TRIS · HCl), 0.01 M acetate/acetic acid, 0.005 M sodium dihydrogen phosphate, and universal buffers of 0.01 M each citric acid, sodium dihydrogen phosphate and boric acid. Desired pHs of buffers were adjusted with dilute HCl or NaOH. All buffers contained 0.1 M NaCl.

Dimyristoyl (PC(C14:0)) and dilauroyl (PC(C12:0)) L-phosphatidylcholine (PC) were from Sigma (99%). Dihexadecylphosphate (99%) was from Aldrich. Water was purified with a Barnstead Nanopure system to specific resistance > 15 MΩ-cm. All other chemicals were reagent grade.

PARC model 273 and Bioanalytical Systems BAS-100B electrochemical analyzers were used for cyclic [25] and square wave voltammetry [26]. The three-electrode voltammetric cell featured a saturated calomel electrode (SCE) as reference, a Pt wire as counter electrode, and a basal plane pyrolytic graphite (PG) disk (HPG-99, Union Carbide; geometric $A = 0.2$ cm^2) as working electrode. PG electrodes were abraded with 600-grit SiC paper on a metallographic polishing wheel prior to coating with Mb–surfactant films [5]. The voltammetric cell was thermostated at 25 ± 0.2°C.

2.2. Preparation of Mb–surfactant films

Phosphatidylcholine (PC) vesicle dispersions were prepared [21] by sonicating 5 mM PC suspensions in water until they became clear (~ 24 h). Mb–PC films were prepared on electrodes by two methods. In the first, 10 μl of the 5 mM PC vesicle dispersion was spread with a microsyringe onto a PG electrode and dried in air overnight. This coated electrode was then placed into a buffer solution containing 0.5 mM Mb for incorporation of Mb into the film. In the second method, 10 μl of 0.25 mM Mb in a 2.5 mM PC vesicle dispersion was deposited onto a PG electrode and dried in air overnight. Mb–PC films made by either method gave similar voltammograms. The second method was more convenient and quantitative, and was used for most of the work reported.

Dihexadecyl phosphate (DHP) films were made by casting 10 μl of 0.05 M DHP in chloroform onto PG electrodes. Chloroform was evaporated in air overnight. DHP-coated PG electrodes were then placed into 0.5 mM Mb buffer solution overnight or longer for incorporation of Mb.

2.3. Procedures

Voltammetry on electrodes coated with Mb–surfactant films was carried out in buffers containing no Mb. Buffers were purged with purified nitrogen ≥ 20 min after immersion of the electrode prior to a

series of experiments. A nitrogen environment was kept over solutions in the voltammetric cell at all times. The ohmic drop of the cell was compensated electronically [25], with uncompensated resistance typically 5–7 Ω. Cyclic voltammetry (CV) was used to measure the formal potential $E^{o\prime}$ as the midpoint between the reduction and oxidation peaks [25].

A pH electrode (Fisher) in the electrochemical cell connected to a Corning model 130 pH meter was used to monitor pH. No pH difference was observed before and after CV scans. All changes in CVs with pH were reversible, and no evidence was found for damage of the films during a series of scans in buffers ranging from pH 3 to 11.

UV–Vis absorption spectroscopy was carried out with a Perkin-Elmer Lambda-6 spectrophotometer. For films, vesicle dispersions of 1.7 mM PC in 3.3 mM buffers of the desired pH containing 0.17 mM Mb were used. Films were prepared by depositing this mixture onto quartz slides, and drying in air. Spectra were also taken of 12 μM Mb in 120 μM PC vesicle dispersions in aqueous buffer.

Scanning electron microscopy (SEM) was carried out with an Amray 1810 microscope. Coated electrodes were fixed on the SEM mounting stage by low resistance contact cement (Ernest F. Fullam, Latham, NY). For cross-sectional views, thin PG electrodes were fractured after immersion in liquid nitrogen [27]. Prior to SEM, 5 nm of gold was coated onto samples with a SC 500 sputter coater (Bio-Rad).

3. Results

3.1. Film thickness

In Mb-containing films made with other insoluble surfactants [5,18–20], thicknesses of up to 20 μm were used. Because the PCs are slightly water soluble [23], it was not possible to prepare Mb–PC films of this thickness. Such films became thinner after soaking in buffer for several minutes, but then remained stable on PG electrodes for a month or more. This thinning process could be visualized by scanning electron microscopy (SEM). A film that was about 10 μm thick originally showed an intricate textured appearance in an SEM top view (Fig. 1a). Its average thickness was confirmed by a side view after freeze fracture. After such films were soaked in buffer for 30 min, the SEM appeared very different, consisting of small spots of 0.1–0.3 μm diameter. The thickness of freeze-fractured Mb–PC films on PG electrodes soaked in buffer for 30 min was estimated at 1–2 μm by SEM.

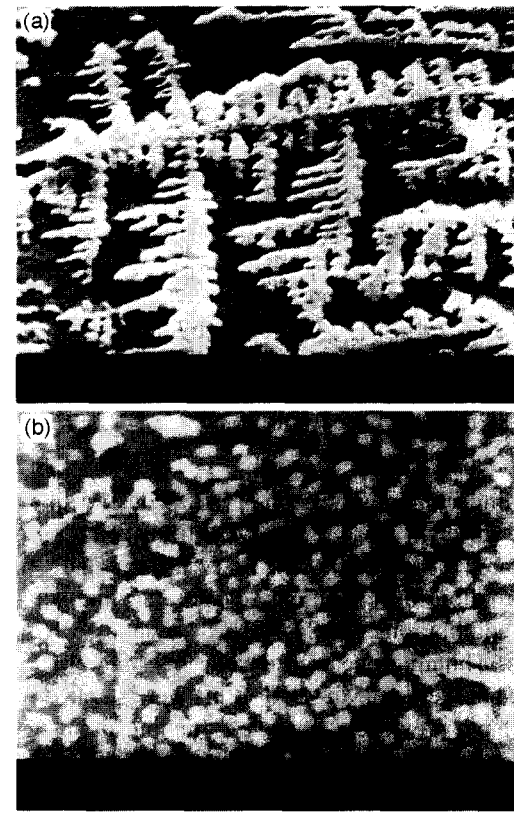

Fig. 1. Top-view SEM images of Mb–PC(C14:0) on a PG electrode. a. Before soaking in pH 5.5 buffer. b. After soaking in buffer for 30 min.

Thinning of Mb–PC films on quartz or glass was observed by absorbance spectroscopy. Immediately after preparation, Mb–PC films gave the typical Soret band at about 409 nm for aquo-metmyoglobin (MbFe(III)–H_2O) [28], similar to that in films of other surfactants [5,20]. However, immersion of films into aqueous buffers led to rapid decreases in absorbance (Fig. 2). After 60 s immersion, the Soret band was barely detectable. Analysis of the solution by measuring the Soret band of dissolved Mb showed that 92% of the Mb deposited in the film had been dissolved in the solution after 30 min. This is consistent with a decrease in film thickness of about 90%.

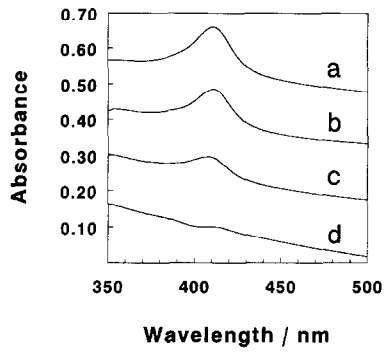

Fig. 2. UV-Vis absorption spectra of Mb–PC (C14:0) films on quartz slides soaked in pH 5.5 buffers for: a, 0; b, 1; c, 8; and d, 60 s. Spectra offset on A-axis for clarity.

Similar thinning was observed for DHP films, but for a different reason. Mb–DHP films could only be prepared successfully by first casting DHP films from chloroform solutions, evaporating the solvent, and equilibrating for 24–48 h in aqueous Mb solutions. Thinning occurred during this long equilibration, but the final Mb–DHP films were stable on PG. We have previously observed thinning of insoluble surfactant films without protein, and believe that it occurs in this case before enough protein has entered the film to stabilize it.

3.2. Cyclic voltammetry

Reproducible CVs for Mb–PC films were obtained within several minutes after immersion in anaerobic buffer. A reversible pair of reduction–oxidation peaks was observed (Fig. 3a) with an average midpoint potential at pH 7 of −320 mV vs. SCE (−78 mV vs. NHE). The shapes of these peaks were nearly symmetric, indicating thin layer electrochemical behavior [25], with equal reduction and oxidation peak heights. This behavior suggests that all of the electroactive MbFe(III) in the film is converted to MbFe(II) on the forward scan to negative potentials, with full conversion of MbFe(II) to MbFe(III) on the reverse scan.

Peak currents for Mb–PC films were linearly proportional to scan rates up to 10 V s^{-1} (Fig. 3b), as expected for thin layer electrochemistry [25,29]. Plots of log peak current vs. log scan rate had correlation coefficients of 0.998 with slopes of 0.96, similar to the theoretical slope of 1 for thin layer voltammetry [29,30]. Mb–PC(C12:0) and Mb–PC(C14:0) films showed identical behavior.

For thin layer cyclic voltammetry, the integral under the reduction curve gives the number of moles of electroactive species in the thin film [25,29,30]. Integration of the CVs of Mb–PC films gave an average surface concentration of electroactive Mb of 2.9×10^{-10} mol cm^{-2}, with a variability of ±10%. A rough estimate of the concentration of electroactive protein in the film from this surface concentration and the film thickness is 2–3 mM.

Useful Mb–DHP films could not be prepared by casting protein–vesicle dispersions (see Section 2). When cast DHP films were placed in Mb solutions, uptake of sufficient protein for voltammetric studies took one to two days, as opposed to < 30 min for PC films. Thus, Mb–DHP films may be less useful than protein films made with other surfactants, and were examined in less detail. Nevertheless, their properties are of interest as an example of an anionic surfactant film existing in the solid-like gel state at ambient temperature [21].

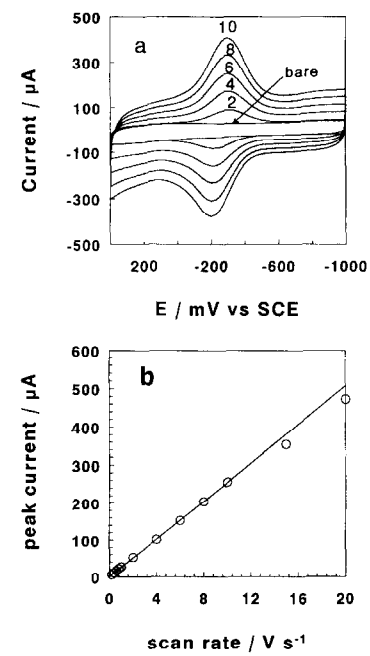

Fig. 3. Representative cyclic voltammograms for Mb–PC(C14:0) films in pH 5.5 buffer containing 0.1 M NaCl, but no Mb. a. Films at scan rates of 2–10 V s^{-1}. Curve marked "bare" is for bare PG electrode in 0.25 mM Mb solution. b. Influence of scan rate on reduction peak current.

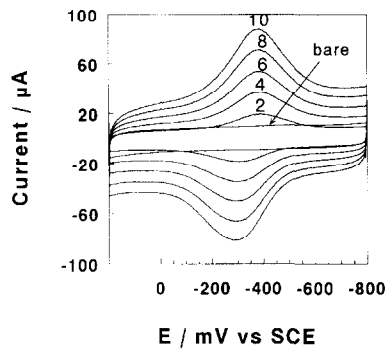

Fig. 4. Representative cyclic voltammograms for Mb–DHP films in pH 7.5 buffers containing 0.1 M NaCl, but no Mb: films at scan rates of 2–10 V s^{-1}; curve marked "bare: is for bare PG electrode in 0.25 mM Mb solution.

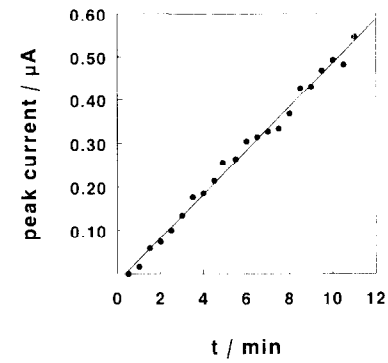

Fig. 5. Increase in MbFe(III) peak current at 0.4 V s^{-1} with time after immersion of a PC(C14:0) film into 0.25 mM Mb in pH 5.5 buffer.

CVs for Mb–DHP films were similar to those of Mb–PC films (Fig. 4), but peak currents were significantly smaller. Symmetric peak shapes and linear proportionality of peak current to scan rate again indicate reversible thin layer voltammetry. Integrations of CVs gave an average surface concentration of electroactive Mb of 0.39×10^{-10} mol cm^{-2}, with a variability of $\pm 10\%$.

The time of protein penetration into pure surfactant films was investigated to obtain information about mobility within the films. Penetration experiments were done by placing electrodes coated with protein-free surfactant films into 0.25 mM Mb solutions at pH 5.5, and using CV to monitor the growth of the MbFe(III) peak. After PC films were placed into Mb solutions, peak currents began to increase (Fig. 5) after about 30 s. This suggests that Mb physically passed through the PC film and was reduced at the electrode. This process probably occurs simultaneously with partial film dissolution, as mentioned above.

When DHP films on PG were placed into Mb solutions, no evidence of Mb penetration through the film was found over two hours. MbFe(III) peaks appeared only after overnight soaking. This is consistent with very slow protein transport in the solid-like gel phase of DHP films at ambient temperature [21].

3.3. Electron transfer kinetics

As scan rate is increased, the separation between CV reduction and oxidation peaks (ΔE_p) increases because of limiting electron-transfer kinetics (Fig. 6). Values of ΔE_p were used to estimate rate constants for electron transfer between electrodes and Mb by the method of Laviron [30,31]. The Laviron model assumes identical, non-interacting electroactive centers on the electrode.

For all Mb films, $\Delta E_p < 200$ mV, and Eq. (1) (from Fig. 4 of Ref. [31]), assuming an electrochemical transfer coefficient (α) of 0.5, was used to obtain apparent surface electron transfer rate constants (k_s)

$$1/m = 1.459 \times 10^{-2} + 2.335 \times 10^{-2}\Delta E_p + 1.323 \times 10^{-4}\Delta E_p^2 + \ldots \quad (1)$$

where $m = (RT/F)(k_s/n\nu)$, R is the gas constant, T is absolute temperature, F is Faraday's constant, n is the number of electrons transferred per protein molecule (here $n = 1$), and ν is the scan rate.

Results in Table 1 show an increase in k_s as the

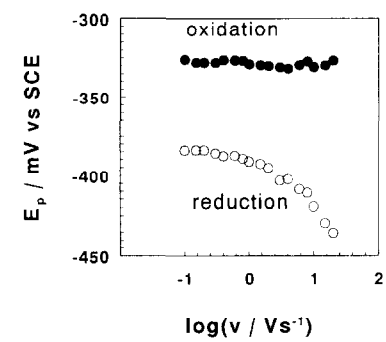

Fig. 6. Influence of scan rate on reduction and oxidation peak potentials for a Mb–PC(C14:0)–PG film at pH 7.0.

Table 1
Scan rate dependence of surface electron transfer rate constants obtained from CV by the Laviron method [a]

Scan rate/V s^{-1}	k_s/s^{-1}			
	Mb–PC(C14:0) films, pH 5.5	Mb–PC(C14) films, pH 8	Mb–PC(C12:0) films, pH 5.5	Mb–PC(C12:0) films, pH 8
2	23 ± 1	32 ± 2	31 ± 2	36 ± 2
4	46 ± 4	57 ± 2	57 ± 3	64 ± 2
6	70 ± 7	83 ± 2	82 ± 6	90 ± 3
8	87 ± 5	102 ± 2	107 ± 10	111 ± 5
10	104 ± 9	121 ± 3	126 ± 12	134 ± 7

[a] See Refs. [30,31].

scan rate is increased. This behavior was observed for k_s from CV data in various buffers and at several pH values, as well as for Mb–DHP films. It is not caused by uncompensated ohmic drop in the electrochemical cell, since this would bias k_s in the opposite direction to that observed. Clearly, the ideal Laviron model does not adequately fit CV data for these films. Similar scan-rate-dependent k_s values were reported for cytochrome c adsorbed onto tin oxide electrodes [32] and for cytochrome c covalently attached to self-assembled monolayers on electrodes [33].

3.4. Square wave voltammetry (SWV)

In this pulsed voltammetric method, the potential waveform applied to the electrochemical cell consists of a symmetric square forward and backward pulse sequence superimposed on a staircase potential ramp [26]. The resulting current at the end of each forward and backward pulse is measured. SWV has distinct advantages in signal-to-noise and resolution over CV, often making it a better choice for quantitative fitting of models to voltammetric data [26].

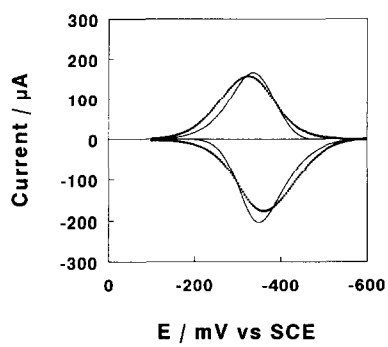

Fig. 7. Square wave forward and reverse current voltammograms for Mb–PC(C14:0)–PG electrodes in pH 7.5 buffers. Points represent the experimental background-subtracted SWV; the solid line was fitted by using nonlinear regression analysis with a model for a single species confined to the electrode surface [34]. SWV conditions: frequency, 140 Hz; pulse height, 75 mV; step height, 4 mV.

Theory was recently developed for SWV for species confined to an electrode surface [34]. When this model was fit onto experimental SWVs for Mb–PC or Mb–DHP films, peaks in both forward and reverse current vs. potential curves were much broader than the theoretical shapes (Fig. 7). Fitting was unsuccessful for this reason.

The broadening of a voltammetric peak suggests possible thermodynamic or kinetic dispersion. This has been attributed to repulsion between reactants [30,35–37], differences in the spatial distribution of the redox centers [38,39], and a dispersion of formal potentials ($E^{o\prime}$) [40–44]. Here we consider dispersion of $E^{o\prime}$ values as a realistic model for Mb heme centers dispersed in films at a relatively low density, consistent with the 0.1–3 mM protein concentrations in these films. The model implies different classes of Mb molecules in the films with slightly different $E^{o\prime}$ values. Combining the $E^{o\prime}$-dispersion model with the theoretical treatment for SWV of a confined species [34], the observed current (i) is given by

$$i = \sum_j i_j \tag{2}$$

where i_j is the contribution of the jth class of redox centers with formal potential $E_j^{o\prime}$ to the total current, given by

$$i_j = \left(nFA\Gamma_j^*\right)\frac{\Psi_j}{t_p} \tag{3}$$

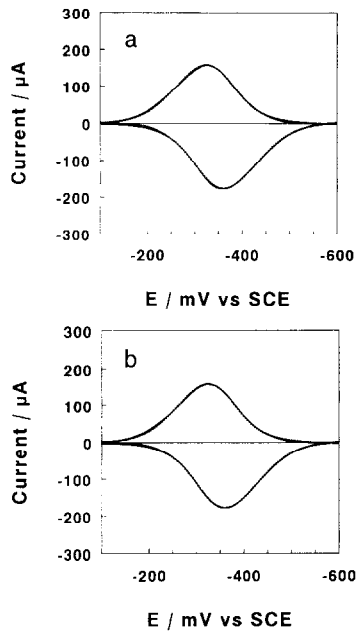

Fig. 8. Square wave forward and reverse current voltammograms for Mb–PC(C14:0)–PG electrodes in pH 7.5 buffers fitted by using the $E^{o\prime}$-dispersion model Eqs. (2)–(7) with: a, 7-$E^{o\prime}$'s; and b, 10-$E^{o\prime}$'s. Points represent the experimental background-subtracted SWV; the solid line was the best fit to the model by nonlinear regression analysis. SWV conditions: frequency, 140 Hz; pulse height, 75 mV; step height, 4 mV.

where n is the number of electrons transferred per redox center, A is electrode area (cm^2), Γ_j^* is the total surface concentration (mol cm^{-2}) of the jth class, and t_p is the pulse width. Ψ_j is the dimensionless current described as

$$\Psi_j = \left[(\kappa_{f,j} + \kappa_{b,j})\Gamma'_{o,j} - \kappa_{b,j}\right]\exp\left[-(\kappa_{f,j} + \kappa_{b,j})\right] \quad (4)$$

and

$$\Gamma''_{o,j} = \frac{\Psi_j + \kappa_{b,j}}{(\kappa_{f,j} + \kappa_{b,j})} \quad (5)$$

where $\Gamma'_{o,j}$ is the jth surface concentration ratio $\Gamma_{o,j}/\Gamma_j^*$ at time $t = 0$, $\Gamma''_{o,j}$ is the ratio $\Gamma_{o,j}/\Gamma_j^*$ at $t = t_p$, $\kappa_{f,j} = k_{f,j}t_p$ and $\kappa_{b,j} = k_{b,j}t_p$. Rate constants k_f and k_b are for forward and backward electron transfer as in the Butler–Volmer equation [25], defined by

$$k_{f,j} = k_s t_p \exp\left[-\alpha(nF/RT)(E - E_j^{o\prime})\right] \quad (6)$$

and

$$k_{b,j} = k_s t_p \exp\left[(1-\alpha)(nF/RT)(E - E_j^{o\prime})\right] \quad (7)$$

where k_s is the standard surface rate constant in s^{-1}, α is the electrochemical transfer coefficient, E is applied potential, $E_j^{o\prime}$ is the standard potential of the jth class of redox centers, and R, T, and F are defined as in Eq. (1). Voltammograms were computed by applying Eqs. (2)–(7) repetitively, using average k_s and α values. A detailed description of these computations and their errors will be published elsewhere [45].

$E^{o\prime}$-dispersion models with 2 to 10 classes of redox centers were tested. Fitting to SWV data was done by nonlinear regression using a general program employing the Marquardt–Levenberg algorithm [46]. Potentials were considered to be error-free, and errors in current were assumed to be constant. The parameters for the regression analysis were Γ_{tot}^*, average α, average k_s and the collection of m $E_j^{o\prime}$ values, where m is the number of classes of redox centers in the film. While the quality of the

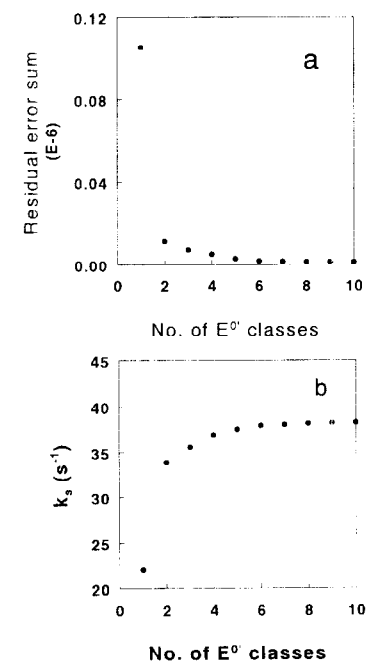

Fig. 9. Influence of the number of $E^{o\prime}$ classes in the SWV model on: a, residual error sums (S) from the regression analyses; b, average electron transfer rate constants. SWV conditions: frequency, 140 Hz; pulse height, 75 mV; step height, 4 mV.

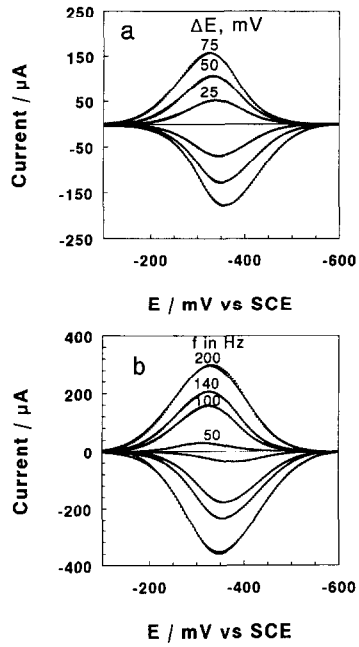

Fig. 10. Square wave forward and reverse current voltammograms for Mb–PC(C14:0)–PG in pH 7.5 Tris-buffer containing 0.1 M NaCl at step height 4 mV. Points represent the experimental background-subtracted SWV; solid lines are the best fits to the 7-$E^{o\prime}$ model by nonlinear regression analysis: a, frequency, 100 Hz; pulse heights (ΔE) in mV given on curves: b, pulse height, 75 mV; frequencies given on curves.

fit improved with the increasing number of E^{o}'s, optimum fits were reached at ≥ 7 classes. Voltammograms fitted with seven-$E^{o\prime}$ and ten-$E^{o\prime}$ models gave similar results (Fig. 8).

Residual error sums (S) and rate constants (k_s) from the regression analyses reached nearly constant values at $m \geq 7$ (Fig. 9). The values of average formal potential ($E^{o\prime}_{avg}$), Γ^{*}_{tot}, and α did not vary significantly with m for $m \geq 7$.

The extra-sum-of squares F-test [46] was used as an additional statistical test to judge the model giving the best fit. The individual regression models to be compared have different numbers of parameters (p). The extra-sum-of-squares F-test accounts for this difference. It involves calculating the F ratio

$$F(p_2 - p_1, n - p_2) = \frac{(S_1 - S_2)/(p_2 - p_1)}{S_2/(n - p_2)} \qquad (8)$$

where S_1 and S_2 are the residual error sums from regression analyses of the same data onto models 1 and 2, p_1 and p_2 represent the numbers of parameters in each model, and the subscripts refer to the specific models. The F statistic is calculated from Eq. (8) after the regression analyses. Comparison with statistical F-tables revealed that there was no significant difference between the $m = 9$ and $m = 10$ models when fitting experimental data, but the models fit less well as m became ≤ 8. However, differences in goodness of fit for $7 \leq m \leq 10$ were marginal, and parameter values for these fits differed by $< 1\%$. Thus, except where indicated, the $m = 7$ model was used for all data discussed below as a compromise between goodness of fit and ease of computation.

The $7 - E^{o\prime}$ model gave good fits to experimental square wave voltammograms of Mb–surfactant films at various pulse heights and frequencies (Fig. 10). $E^{o\prime}_{avg}$ and α were essentially constant for data obtained under different experimental conditions. The rate constant k_s did not depend on frequency at pulse heights of 50 and 75 mV. At pulse height 25 mV, k_s increased slightly with increasing frequency, similar to the way in which k_s estimated from CV data increased with increasing scan rate.

Table 2
Electrochemical parameters of Mb–lipid films at pH 7.5 from nonlinear regression analysis of SWV onto seven-$E^{o\prime}$ model [a]

Film	$E^{o\prime}_{avg}$ (mV vs. NHE)		α	k_s/s^{-1}	$\Gamma^{*}_{tot} \times 10^{10}$/mol cm^{-2}	
	SWV	CV			SWV	CV [d]
Mb–PC(C14:0) [b]	-100 ± 1	-110 ± 3	0.50 ± 0.02	35 ± 6	3.4 ± 0.7	2.9
Mb–DHP [c]	-89 ± 5	-98 ± 6	0.52 ± 0.02	90 ± 7	0.5 ± 0.1	0.4

[a] In pH 7.5 Tris-buffer containing 0.1 M NaCl. [b] Average values obtained from 12 SWVs at 50–75 mV pulse heights and $f = 100$–200 Hz data. [c] Average values obtained from 10 SWVs at 50–75 mV pulse heights and $f = 300$–500 Hz. [d] By integrating CV reduction peaks, $\pm 10\%$ relative standard deviation.

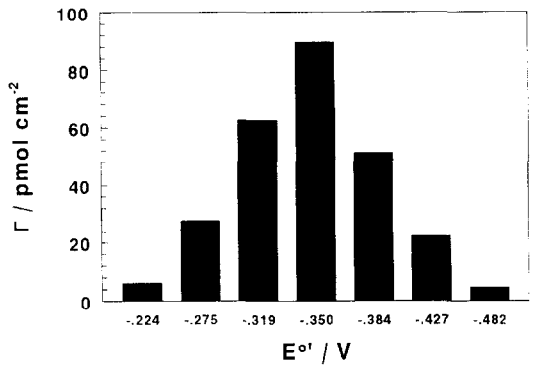

Fig. 11. Distribution of amounts of Mb in Mb–PC(C14:0) film expressed as surface concentrations with different $E^{o\prime}$-values from analysis of SWV with model having 7-E^{o}'s and their associated Γ_j^*: pulse height, 75 mV; frequency, 100 Hz; step height, 4 mV.

Table 3
Influence of pH on parameters from CV [a] on pH for Mb–PC(C14:0) films

pH	i_{pc} / μA	$\Gamma_{tot}^* \times 10^{10}$ / mol cm^{-2}	E_{FWHM} / mV	$E^{o\prime}$/mV/ NHE	ΔE_p / mV
10.9	53.5	2.6	163	−332	40
9.9	48.6	2.5	178	−268	64
9.0	43.5	2.4	189	−210	83
8.0	40.1	2.5	220	−144	90
7.0	41.6	2.6	220	−92	87
7.0	41.6	2.5	210	−85	81
6.0	38.6	2.4	222	−28	85
6.0	39.6	2.5	220	−28	82
5.0	41.4	2.6	220	14	78
4.0	48.6	2.7	193	46	71
3.2	54.7	2.7	172	59	63

[a] Scan rate, 2 V s^{-1}.

Despite these errors in k_s at small pulse heights, the $E^{o\prime}$-dispersion model for SWV at pulse heights ≥ 50 mV gave satisfactory fits to SWVs for Mb–surfactant films. A summary of results for Mb–PC(C14:0) and Mb–DHP films is given in Table 2.

Another mode of fitting with the $E^{o\prime}$-dispersion model was briefly examined in which both 7-E^{o}'s and their associated Γ_j^* were used as fitting parameters. The additional parameters increased analysis time 2-fold, but the quality of fits was comparable to those in Fig. 10. Rate constants found were within ±2% of those with the simpler analysis using the global Γ_{tot}^* parameter. When using all the Γ_j^* as parameters, the distribution of E^{o}'s is revealed. These distributions were roughly Gaussian (Fig. 11).

To see if the SWV parameters could explain the CV results, we computed CVs from parameters obtained from fits using 7-E^{o}'s and their associated Γ_j^*. A summed Gaussian peak model [46] (one peak for each $E^{o\prime}$) using the parameters estimated from SWV reproduced the CV peak shapes. In particular, widths for calculated peaks were in good agreement with experiment (200 ± 20 mV) between 0.5 and 10 V s^{-1}.

3.5. Dependence on pH for Mb–PC films

All changes in CV peak potentials and currents with pH were reversible. Electrochemical properties of Mb–PC films at pH 7 were recovered even after exposure to pH 3 buffer, where Mb is partly denatured [47–49]. Typical results are shown for an Mb–PC(C14:0) film (Table 3). The reversibility of the films when changing pH is demonstrated by the duplicate entries for pH 6 and 7, one set of which was obtained before and one after CVs at all the other pHs were measured.

Plots of formal potentials vs. pH were linear between pH 5 and 11 with slopes of −60 mV/pH (Fig. 12). This suggests that a single proton transfer is coupled to the electron transfer reaction [50,51]. There is an inflection point in the plot at about pH 4.6, and at lower pH the formal potential is nearly pH-independent.

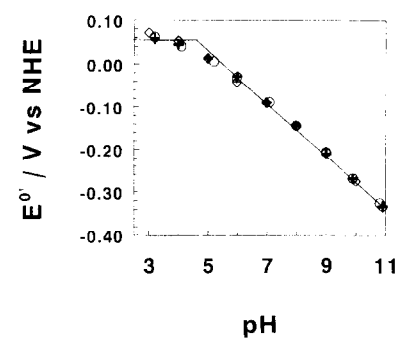

Fig. 12. pH Dependence of formal potential: +, Mb–PC(C14:0) in phosphate buffers; ○, Mb–PC(C12:0) in phosphate buffers; ◇, Mb–PC(C14:0) in universal citrate/phosphate/borate buffers. All buffers contained 0.1 M NaCl.

Total surface concentrations (Γ_{tot}) were independent of pH within the error of integration of the CVs, suggesting that the amount of electroactive Mb in the films is roughly independent of pH. Separations of reduction and oxidation peaks (ΔE_p), which are inversely related to electron transfer rates [30], were essentially constant between pH 5 and 9, and decreased at lower and higher pHs. The voltammetric peak width at half-height (E_{FWHM}) at pH 7.0 is about 50–60 mV larger than that at pH 3.2 and 10.9.

As seen in Fig. 2, Mb–PC films are not sufficiently stable on quartz for detailed spectroscopic studies in buffers. However, freshly prepared films were exposed to the buffer solution for a few seconds without extensive dissolution. The pH dependence of Soret band spectra of the heme groups of Mb in buffer, in PC films and in PC vesicle dispersions, were compared. Between pH 5 and 7, the Mb Soret band was at 408–409 nm in buffers [52–54] and PC vesicles (Fig. 13). Mb–PC films had a Soret band at 410 nm in this same pH range. Partial acid-induced denaturation of Mb in PC films, vesicle dispersions and aqueous solutions caused the Soret peak to shift blue, as observed previously in solution [52–55].

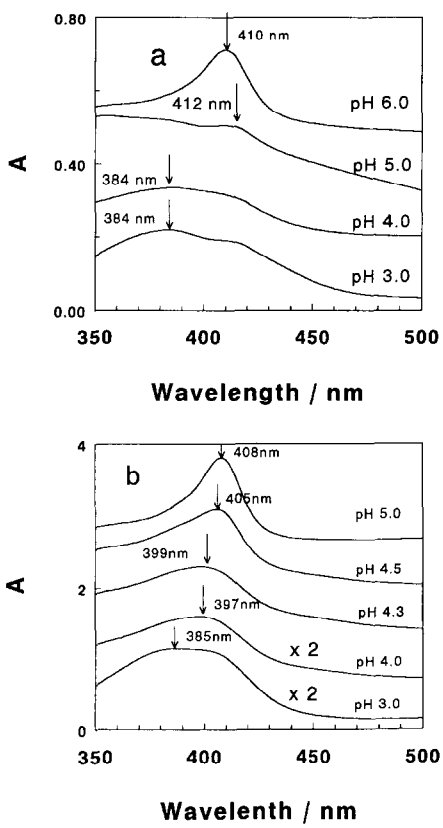

Fig. 13. Absorption spectra of Mb Soret region. a. Mb–PC(C14:0) films on quartz slides. b. 12 μM Mb in PC (C14:0) vesicle dispersions. Spectra are offset on A-axis for clarity.

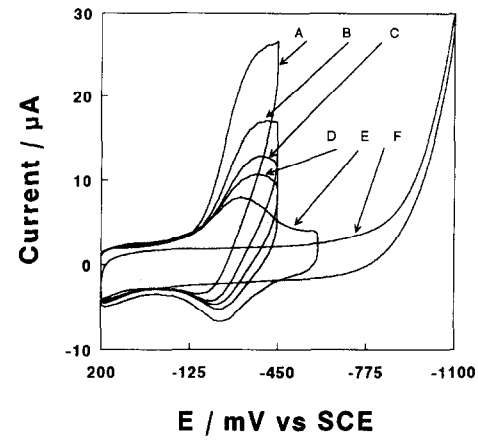

Fig. 14. Cyclic voltammograms at 100 mV s^{-1} in pH 5.5 buffer containing 0.1 M NaCl. Curves A–E are for Mb–PC(C14:0)–PG electrode in buffers containing trichloroacetic acid at: A, 20 mM; B, 8 mM; C, 4 mM; D, 2 mM; and E, 0 mM. Curve F is for PC(C14:0)–PG electrode without Mb in buffer containing 5 mM trichloroacetic acid.

Some differences in spectra of Mb in PC vesicle dispersions and Mb solutions were noted at low pH. The Soret band in buffers shows an abrupt decrease between pH 5 and 4.3 and the maximum shifted to 405 nm due to the partial unfolding of Mb [34–36]. Solution spectra at pH 4 and 3 were almost identical, showing a broad absorption at about 370 nm. In vesicle dispersions (Fig. 13b), absorbance decreased gradually from pH 5.0 to 4.0 accompanied by a blue shift from 408 to 397 nm. At pH 3.0, a broad double peak with maxima at about 397 and 385 nm was found. Spectra in Mb–PC films (Fig. 13a) are more similar to those in the vesicle dispersions than in aqueous buffers.

3.6. Catalysis

Electrochemical catalytic activity of Mb–PC films was tested by CV for the reduction of trichloroacetic

acid, with which MbFe(II) reacts [22]. When trichloroacetic acid was added to the buffer, an increase in the Mb Fe(III)/Fe(II) reduction peak in Mb–PC films was observed (Fig. 14). This was accompanied by disappearance of the MbFe(II) oxidation peak as the trichloroacetic acid concentration was increased. These results indicate reaction of MbFe(II) with trichloroacetic acid in a catalytic cycle, presumably resulting in the reductive dechlorination of the acid [22]. The peak reduction current for Mb increased with increasing trichloroacetic acid concentration in solution, characteristic of electrochemical catalysis [25].

4. Discussion

4.1. Film morphology and electron transfer properties

SEM (Fig. 1), time dependence of absorbance spectroscopy (Fig. 2) and thin-layer voltammetric behavior (Figs. 3 and 4) of the Mb–PC and Mb–DHP films are consistent with thinning processes which leave stable films of 1–2 μm on electrodes. SEM of Mb–PC showed (Fig. 1b) that the final films on PG are not uniform, but apparently consist of islands 0.1–0.3 μm in diameter spaced rather closely on the PG surface.

For Mb–PC films, rapid thinning when the films are exposed to water is probably a consequence of the slight water solubility of the PCs, leaving a thin stable layer adhering to the PG. Similar thinning occurs for films of Mb and didodecyldimethylammonium bromide exposed to microemulsions [56]. For the DHP films, thinning occurs during the one- or two-day exposures to Mb solutions necessary to incorporate the protein. In this case, the eventual inclusion of Mb seems to stabilize the films, as also found for other surfactants [5].

As in films of other surfactants [5,18–20], electron transfer between the electrode and Mb is greatly facilitated in PC and DHP films. While reversible electron transfer was observed in both types of films, no evidence for electron transfer was found at PG electrodes in ultrafiltered Mb solutions (Fig. 3 and Fig. 4). In fact, direct electron transfer between Mb in solution and PG has been observed only in extremely pure Mb solutions [18], and it is much slower than that reported here.

The ideal Laviron model did not fit voltammetric data for Mb–PC and Mb–DHP films. This was shown by the dependence of the estimated rate constant on scan rate (Table 1), and also by the unsymmetric shift of oxidation and reduction peak potentials as scan rate increased (Fig. 6). The Laviron model predicts symmetric shifts of these two peaks in opposite directions as scan rate increases [30,31]. A similar model [34] failed to fit square wave voltammograms of the films (Fig. 7).

An extension of the SWV model for surface-confined redox centers assuming a distribution of redox centers with slightly different $E^{o\prime}$ values gave excellent fits to the data for pulse heights ≥ 50 mV and frequencies of 50–200 Hz (Fig. 8 and Fig. 10). Models using 7 to 10 redox classes gave similar results (Fig. 8 and Fig. 9). The success of this model suggests a distribution of Mb molecules in the films with slightly different redox properties.

The $E^{o\prime}$-dispersion model is a definite improvement over the simple Laviron or single-$E^{o\prime}$ models for electrochemistry of protein–lipid films. However, poorer results at pulse heights < 50 mV suggest that further refinements may be necessary to generalize the model for these films. It is relevant that for noisy theoretical data we observed fitting results at pulse heights < 50 mV that were consistent with those at larger pulse heights. This suggests that the problem lies in fully describing the experimental system, and not in the mathematical procedures. At the same time, we conclude that analysis of SWV results at pulse heights > 50 mV with the $E^{o\prime}$-dispersion model gives an adequate description of the electron transfer kinetics in protein–lipid films as evidenced by the quality of fits (Fig. 10).

The average $E^{o\prime}$ values of Mb in the PC and DHP films found from the analysis of SWV data were similar to those obtained from CV (Table 2). For films in solutions close to pH 7, the $E^{o\prime}$ values are 135–150 mV more negative than the $E^{o\prime}$ of 50 mV vs. NHE for Mb dissolved in pH 7 solution [57]. In films of the cationic surfactant didodecyldimethylammonium bromide (DDAB), $E^{o\prime}$ at pH 7 was 24 mV [58]. In general, the $E^{o\prime}$ values of Mb in such films show a dependence on the type of lipid [20],

suggesting the influence of protein–lipid interactions and/or double-layer effects [25] of the lipid on the electrode potential felt by the redox center.

Electron transfer rate constants found by SWV (Table 2) were 8-fold greater in PC films and 20-fold greater in DHP films than the value of 4 s^{-1} in thin films of DDAB stabilized with the ionomer Nafion [59]. DHP films contain about 7-fold less electroactive protein than the PC films. This may be because the PC's are in the lamellar liquid crystal phase at room temperature, while DHP is in the gel state [21]. In the latter solid-like phase, it is more difficult for the film to accumulate protein [20].

Supramolecular structures of Mb–PC and Mb–DHP films were previously characterized by ESR anisotropy, linear dichroism, and thermal phase transition studies [21]. In pH 5.5–7.5 buffers, Mb retains its native conformation and is specifically oriented in these films. The average orientation of the heme plane to the film normal was $60 \pm 2°$. The observance of gel-to-liquid crystal phase transitions of these films similar to those of bilayer vesicle dispersions of the same surfactants suggested that surfactants in the films are arranged in bilayers similar to those in lipid membranes.

4.2. Dependence of Mb electron transfer on pH in PC films

The dependence of $E^{o\prime}$ and CV peak shape on pH indicates that Mb within the films is sensitive to the pH of the contacting buffer solutions. The -60 mV/pH shift in $E^{o\prime}$ between pH 5 and 11 (Fig. 12) indicates [50,51] that a single protonation accompanies electron transfer between the electrode and the heme Fe(III) of aquometmyoglobin. The voltammetry of Mb in the PC films is thus the result of

$$\mathrm{MbFe(III)} + e^- + \mathrm{H^+} \rightleftharpoons \mathrm{MbFe(II)} \qquad (9)$$

The pH-independent region of the $E^{o\prime}$ plot at pH < 4.6 suggests that the electroactive center is already protonated, and corresponds to the pH range in which the protein is partly unfolded [47–49,52–55]. The Soret band shifts blue in PC films and vesicle dispersions (Fig. 13) in this pH range, also reflecting partial unfolding [49].

NMR studies of horse and sperm whale myoglobin [49,60] showed that distal and proximal histidines are protonated between pH 4.3 and 5, along with four other histidines. The bond between the iron-bound proximal histidine and MbFe(III) may be broken [60,61] below pH 5. It is possible that the protonation coupled to electron transfer in the films at pH 5–11 involves the proximal and/or distal histidine, with an accompanying conformational change [49,60], prior to electron transfer. At pH < 4.6, a protonated, partly unfolded Mb appears to accept electrons directly. Further details of the mechanism of electron transfer to Mb in films of PC and DDAB will be discussed in a separate paper [58].

4.3. Catalysis of trichloroacetic acid reduction

Voltammetric data for the Mb–PC films in solutions containing trichloroacetic acid (Fig. 14) demonstrate electrochemical catalytic reduction of the acid. This reductive dechlorination was investigated in detail in Mb–DDAB films [22]. MbFe(II) created by injection of electrons from the electrode reacts with trichloroacetic acid which has entered the film, giving dichloroacetic acid as the initial product. Thus, Mb–PC films can mimic the enzyme action of membrane-bound cytochrome P450 in anaerobic environments [13–15].

5. Summary

Mb forms stable thin films with pure phosphatidyl cholines or DHP, giving reversible electron transfer with electrodes. The PC films are lamellar liquid crystalline at room temperature and incorporate much more protein than the DHP films, which are in the gel state.

A model assuming thin-layer electrochemical behavior with a distribution of slightly different electroactive sites successfully fit the square wave voltammetric data. The pH dependence of formal potentials of Mb in the PC films suggests that protonation and possibly conformational change, accompanies electron transfer to MbFe(III) between pH 5 and 11. Mb in PC films was used to catalyze the reduction of trichloroacetic acid.

Acknowledgements

This publication was supported by U.S. PHS grant No. ES03154 from the National Institute of Environmental Health Sciences (NIEHS), NIH. Its contents are solely the responsibility of the authors and do not necessarily represent the official views of NIEHS, NIH.

References

[1] P.R. Ortiz de Montellano and C.E. Catalano, J. Biol. Chem., 260 (1985) 9265–9271.
[2] D.J. Kelman, J.A. DeGray and R.P. Mason, J. Biol. Chem., 269 (1994) 7458, and references cited therein.
[3] R.S. Wade and C.E. Castro, J. Am. Chem. Soc., 95 (1973) 231.
[4] E.W. Bartnicki, N.O. Belser and C.E. Castro, Biochemistry, 17 (1978) 5582–5586.
[5] J.F. Rusling and A.-E.F. Nassar, J. Am. Chem. Soc., 115 (1993) 11891.
[6] F.P. Guengerich, and T.L. MacDonald, Acc. Chem. Res., 17 (1984) 9.
[7] J.H. Dawson and M. Sono, Chem. Rev., (1987) 1255–1276.
[8] S. Li and L.P. Wackett, Biochemistry, 32 (1993) 9355.
[9] E.S.R. Newman, C.A. Rice-Evans and M.J. Davies, Biochem. Biophys. Res. Commun., 179 (1991) 1414.
[10] G. Dee, C. Rice-Evans, S. Obeyesekara, S. Meraji, M. Jacobs and K.R. Bruckdorfer, FEBS Lett., 294 (1991) 38.
[11] A. Mikkelsen, L. Sosniecki and L.H. Skibsted, Z. Lebensm. Uniters. Forsch., 195 (1992) 238.
[12] S.I. Rao, A. Wilks, M. Hamberg and P.R. Ortiz de Montellano, J. Biol. Chem., 269 (1994) 7210, and references cited therein.
[13] P.R. Ortiz de Montellano (Ed.), Cytochrome P450, Plenum, New York, 1986.
[14] J.B. Schenkman and H. Greim (Eds.), Cytochrome P450, Springer-Verlag, Berlin, 1993.
[15] T. Omura, Y. Ishimura and Y. Fujii-Kuriyama (Eds.), Cytochrome P450,, VCH Publishers, Tokyo, 1993.
[16] I. Taniguchi, K. Watanabe, M. Tominaga and F.M. Hawkridge, J. Electroanal. Chem., 333 (1992) 331.
[17] M. Tominaga, T. Kumagai, S. Takita, and I. Taniguchi, Chem. Lett., (1993) 1771.
[18] A-E.F. Nassar, W.S. Willis and J.F. Rusling, Anal. Chem., 67 (1995) 2386.
[19] J.F. Rusling and A-E.F. Nassar, Langmuir, 10 (1994) 2800.
[20] A-E.F. Nassar, Y. Narikiyo, T. Sagara, N. Nakashima, and J.F. Rusling, J. Chem. Soc., Faraday Trans., 91 (1995) 1775.
[21] A-E.F. Nassar, Z. Zhang, V. Chynwat, H.A. Frank, J.F. Rusling and K. Suga, J. Phys. Chem., 99 (1995) 11013.
[22] A-E.F. Nassar, J.M. Bobbitt, J.D. Stuart and J.F. Rusling, J. Am. Chem. Soc., 117 (1995) 10986.
[23] G. Cevc and D. Marsh, Phospholipid Bilayers, Wiley, New York, 1987.
[24] A. Kotyk, K. Janacek and J. Koryta, Biophysical Chemistry of Membrane Function, Wiley, Chichester, U.K., 1988.
[25] A.J. Bard and L.R. Faulkner, Electrochemical Methods, Wiley, New York, 1980.
[26] J. Osteryoung and J.J. O'Dea, in A.J. Bard (Ed.), Electroanalytical Chemistry, Vol. 14, Marcel Dekker, New York, 1986, pp. 209–308.
[27] N. Hu, D.J. Howe, M.F. Ahmadi and J.F Rusling, Anal. Chem., 64 (1992) 3180.
[28] E. Antonini and M. Brunori, Hemoglobin and Myoglobin in their Reactions with Ligands, North Holland, Amsterdam, 1971.
[29] R.W. Murray, in A.J. Bard (Ed.), Electroanalytical Chemistry, Vol. 13, Marcel Dekker, New York, 1984, pp 191–368.
[30] E. Laviron, in A.J. Bard (Ed.), Electroanalytical Chemistry, Vol. 12, Marcel Dekker, New York, 1982, pp 53–157.
[31] E. Laviron, J. Electroanal. Chem., 101 (1979) 19.
[32] J.L. Willit and E.F. Bowden, J. Electroanal. Chem., 221 (1987) 265.
[33] M. Collinson, E.F. Bowden and M.J. Tarlov, Langmuir, 8 (1992) 1247.
[34] J.J. O'Dea and J. Osteryoung, Anal. Chem., 65 (1993) 3090.
[35] E. Laviron, J. Electroanal. Chem., 52 (1974) 395–402.
[36] A.P. Brown and F.C. Anson, Anal. Chem., 49 (1977) 1589.
[37] D.F. Smith, K. William, K. Kuo and R.W. Murray, J. Electroanal. Chem., 95 (1979) 217.
[38] K. Itaya and A.J. Bard, Anal. Chem., 50 (1978) 1487.
[39] F.B. Kaufmann and E.M. Englerm, J. Am. Chem. Soc., 101 (1979) 547.
[40] G.K. Rowe, M.T. Carter, J.N. Richardson and R.W. Murray, Langmuir, 11 (1995) 1797.
[41] E. Sabatani and F.C. Anson, J. Electroanal. Chem., 386 (1995) 111.
[42] W.J. Albery, M.G. Boutelle, P.J. Colby, and A.R. Hillman, J. Electroanal. Chem., 133 (1982) 135.
[43] P.J. Peerce and A.J. Bard, J. Electroanal. Chem., 114 (1980) 89.
[44] M.S. Wrighton, M.C. Pallazzotto, A.B. Bocarsly, J.M. Bolts, A.B. Fischer and L. Nadjo, J. Am. Chem. Soc., 100 (1978) 7264.
[45] Z. Zhang and J.F. Rusling, in preparation.
[46] J.F. Rusling and T.F. Kumosinski, Nonlinear Computer Modeling of Chemical and Biochemical Data, Academic Press, New York, 1996.
[47] Y. Goto and A.L. Fink, J. Mol. Biol., 214 (1990) 803.
[48] D. Stigter, D.O.V. Alonso and K.A. Dill, Proc. Natl. Acad. Sci. USA, 88 (1991) 4176.
[49] A.-S. Yang and B. Honig, J. Mol. Biol., 237 (1994) 602.
[50] L. Meites, Polarographic Techniques, 2nd edn., Wiley, New York, 1965, pp. 278–284.
[51] A.M. Bond, Modern Polarographic Methods in Analytical Chemistry, Marcel Dekker, New York, 1980, pp. 27–34.
[52] H. Theorell and A. Ehrenberg, Acta Chem. Scand., 5 (1951) 823.
[53] P. George and G. Hanania, Biochem. J., 52 (1952) 517.

[54] T.T. Herskovits and H. Jaillet, Science, 163 (1969) 282.
[55] M. Brunori, G.M. Giacometti, E. Antonini and J. Wyman, J. Mol. Biol., 63 (1972) 139.
[56] A.C. Onuoha and J.F. Rusling, Langmuir, 11 (1995) 3296.
[57] B.C. King, F.M. Hawkridge and B.M. Hoffman, J. Am. Chem. Soc., 114 (1992) 10603.
[58] A.-E. Nassar, Z. Zhang, J.F. Rusling and T.F. Kumosinski, J. Phys. Chem., submitted.
[59] Q. Huang, Z. Lu and J.F. Rusling, Langmuir, in press.
[60] D. Bashford, D.A. Case, C. Dalvit, L. Tennant and P.E. Wright, Biochemistry, 32 (1993) 8045.
[61] H.-L. Tang, B. Chance, A.G. Mauk, L.S. Powers, K.S. Reddy and M. Smith, Biochem. Biophys. Acta, 1206 (1994) 90.